Synthetic condition to generate magnesium-related acceptor levels in silicon

Matsumoto, Koichi ; Uenaka, Yuki ; Seto, Yusuke ; Yashiro, H ; Nakamura, Hiroyuki ; Kimura, Tsuyoshi ; Uchino, Takashi

(Citation)
JOURNAL OF APPLIED PHYSICS,108(11):113706-113706

(Issue Date)
2010-12-01

(Resource Type)
journal article

(Version)
Version of Record

Synthetic condition to generate magnesium-related acceptor levels in silicon

K. Matsumoto,[1] Y. Uenaka,[1] Y. Seto,[2] H. Yashiro,[3] H. Nakamura,[4] T. Kimura,[4] and T. Uchino[5,a)]
[1]*Department of Chemistry, Faculty of Science, Kobe University, Kobe, Hyogo 657-8501, Japan*
[2]*Department of Earth and Planetary System Sciences, Kobe University, Kobe, Hyogo 657-8501, Japan*
[3]*Application Laboratory, Rigaku Co., Akishima, Tokyo 196-8666, Japan*
[4]*Division of Materials Physics, Graduate School of Engineering Science, Osaka University, Toyonaka, Osaka 560-8531, Japan*
[5]*Department of Chemistry, Graduate School of Science, Kobe University, Kobe, Hyogo 657-8501, Japan*

(Received 10 September 2010; accepted 21 October 2010; published online 6 December 2010)

It has generally been recognized that Mg gives rise to an interstitial donor level in Si although the possibility of the existence of a Mg substitutional acceptor in Si has been suggested. In this work, we explore the synthetic conditions required to obtain substitutional Mg acceptor in Si. We have diffused Mg into Si wafers under the Mg vapor environment created by the thermal decomposition of MgB_2. The Mg vapor pressure is low enough to suppress the formation of the stable silicide phase, Mg_2Si, but is high enough to induce Mg diffusion into Si. The resultant Mg-diffused Si exhibited degenerate *p*-type semiconducting behavior. It was proposed that the presence/absence of the Mg_2Si phase plays a key role in determining the location and solubility of Mg in Si. © *2010 American Institute of Physics*. [doi:10.1063/1.3517412]

I. INTRODUCTION

Impurity states in semiconductors, most especially in silicon, have been one of the well-studied topics in solid-state physics. In contrast to group-III and group-V impurities, however, group-II impurities have attracted less attention because of their generally low solubility ($\sim 10^{15}$ cm^3) in silicon. In addition, there have been no "site-preference" rules concerning the lattice sites of group-II elements in silicon, which leads to perplexing situations in designing *p*- and *n*-type semiconductors. For example, Be (Refs. 1 and 2) and Zn (Refs. 3 and 4) have been reported to give rise to accepter levels, whereas Mg (Refs. 5–11) results mostly in donor levels. As pointed out previously, however, there is no *a priori* reason why Mg should not occupy substitutional sites in silicon.[12] Indeed, both experimental[12] and theoretical[13] results gave implications for the existence of substitutional Mg acceptor sites, suggesting that a desired impurity site can be "engineered" by subtle manipulation of experimental conditions.[12]

The purpose of this study is to investigate the preparing condition to obtain a substitutional Mg acceptor level in Si. We thermally treated Si wafers under a low Mg vapor pressure ($\sim 10^{-3}$ bar) induced by the thermal decomposition of MgB_2. We found that this procedure allows us to introduce a high concentration of acceptor levels in Si, yielding the *p*-type silicon with a resistivity of $\sim 10^{-4}$ Ω cm at room temperature. It should be noted that the resistivity of the thus prepared Si sample decreases with decreasing temperature, showing a typical characteristic of degenerate semiconductors. On the other hand, the thermal treatment of Si under a high Mg vapor pressure (~10 bar) resulted in Mg donor levels, as inferred from the previous reports.[5–11] The observed effect of the Mg vapor pressure is understood in terms of the presence/absence of the Mg_2Si phase during the thermal diffusion process of Mg.

II. EXPERIMENTAL DETAILS

In most of the previous studies, Mg was incorporated into Si by thermal diffusion using the sandwich technique;[5–7,11] that is, an undoped silicon sample is sandwiched between two other specimens, all three having thick magnesium film deposited on the surfaces by evaporation, and heated at ~1200 °C in an inert atmosphere. This technique is useful to prevent magnesium from escaping into the ambient since the sample and the "covers" weld together by forming Mg_2Si,[6] which is the only stable compound in the Mg–Si system. We, however, consider that the formation of Mg_2Si is not preferable in the viewpoint of Mg doping, as will be discussed in Sec. IV. Also, this technique results solely in interstitial donor levels of Mg, as noted earlier.

Thus, we carry out thermal diffusion of magnesium in such a condition as to avert the formation of Mg_2Si. We found that this condition is achieved when Si is heated in the presence of MgB_2 under an Ar atmosphere. It has been demonstrated that MgB_2 is thermally decomposed into Mg and MgB_4 at temperatures more than ~700 °C.[14] The decomposition process of MgB_2 is written by

$$2MgB_2(s) = Mg(g) + MgB_4(s). \quad (1)$$

Thus, monoatomic magnesium is evaporated during the decomposition of MgB_2.[15] The resulting Mg vapor pressure is estimated to be $\sim 10^{-3}$ bar (Refs. 15 and 16) at temperatures around 1000 °C.

In this work, *p*-type (001) and *n*-type (001) silicon wafers were used as substrates. The resistivities of the original

a)Electronic mail: uchino@kobe-u.ac.jp.

wafers were greater than 10 Ω cm for both the *p*-type and *n*-type samples. In what follows, we will mainly show the results of the *p*-type Si substrate since we obtained basically the same structural and electrical properties for both types of samples. MgB_2 was prepared using the following solid-state reaction of B_2O_3 (99% purity) and Mg (99.9% purity) at 800 °C in an Ar atmosphere:[17,18]

$$4Mg + B_2O_3 = MgB_2 + 3MgO. \quad (2)$$

The resultant MgB_2–MgO composite was put in the alumina crucible, and the Si wafer was located above the alumina crucible. We then heated this set of sample in an Ar atmosphere at 1000 °C for 2 h to induce Mg diffusion into the Si substrate.[19]

X-ray diffraction (XRD) analysis was performed with a x-ray diffractometer (Rigaku, SmartLab) using Cu K_α radiation. High-resolution reciprocal space mapping (RSM) around the (004) lattice point was also performed by using a four-crystal Ge(220) monochromator and a two-crystal Ge(220) analyzer in the triple axis configuration. In this optical setup, the Cu $K_{\alpha 2}$ component was completely suppressed. RSM allows one to distinguish changes in orientation of the lattice planes (mosaicity) from variation in the lattice spacing ($\Delta d/d$).[20] The RSM is usually plotted using the following reciprocal space coordinates q_x and q_z:[21]

$$q_x = 1/d_x = -(2/\lambda)\sin(\omega - 2\theta/2)\sin\theta,$$

$$q_z = 1/d_z = (2/\lambda)\cos(\omega - 2\theta/2)\sin\theta,$$

where λ is the incident x-ray wavelength (Cu $K_{\alpha 1}$, λ = 1.5406 Å), 2θ is the angle between the incident and the diffracted beams, and ω is the angle between the incident beam and the sample surface. In the RSM, the scattered intensity due to changes in lattice spacing is observed along the q_z direction, while mosaicity yields a broadening in the scattered x-ray intensity in the q_x direction.

Cross-sectional analysis was performed with the microarea XRD system on BL10XU at SPring-8 in Hyogo, Japan; the incident x-ray beam was monochromatized to a wavelength of 0.400 085 Å and collimated to 15 μm in diameter. The diffracted beam was detected using a flat imaging plate (IP, Rigaku R-AXIS IV). Composition profile of the cross sectional area was obtained by line-scanning techniques using an electron probe microanalyser (EPMA) (JEOL, JXA-8900) equipped with wavelength dispersive x-ray spectrometers (WDS). WDS analyses were obtained at 15 kV and 20 nA, and the data correction were made by the Bence–Albee method using well characterized natural and synthetic minerals as chemical standards. For the cross-sectional analyses, the Si wafer was embedded into epoxy resin and was sliced into approximately 100 μm thick sections with a diamond-blade. The sections were ground and polished to a thickness of approximately 30 μm.

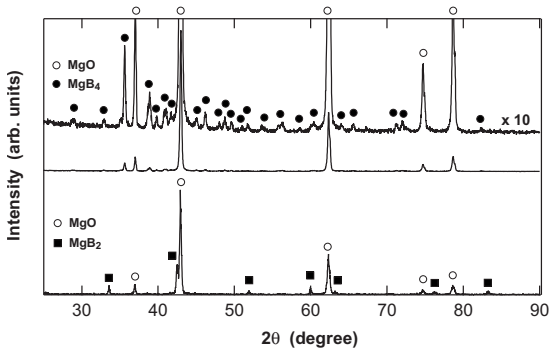

FIG. 1. XRD patterns of the MgO–MgB_2 composite before (bottom) and after (middle and top) heating at 1000 °C for 2 h under an Ar atmosphere.

Electrical resistivity measurements were performed from room temperature down to 7 K using standard lock-in techniques. Gold wires were attached onto the samples in a four-terminal configuration with silver epoxy. Hall measurements were also performed at room temperature in the van der Pauw configuration using a Hall coefficient measurement system (Toyo Corporation, ResiTest 8300).

III. RESULTS

A. XRD analysis

Figure 1 shows the XRD patterns of the starting MgO–MgB_2 composite along with that remained in the crucible after heating at 1000 °C in an Ar atmosphere. The diffraction peaks attributed to MgB_2 disappeared upon heating at 1000 °C and those to MgB_4 newly emerged, in agreement with the decomposition process of MgB_2 described in Eq. (1). Figures 2(a) and 2(b) show the XRD patterns of the (001) Si wafer around the Si(004) diffraction signals ($2\theta \sim 69°$) before and after heat treatment at 1000 °C in the presence of the MgO–MgB_2 composite. The XRD pattern of the original Si wafer [see Fig. 2(a)] is characterized by two Si(004) peaks at $2\theta = 69.18°$ and 69.37°, which correspond to Cu $K_{\alpha 1}$ (λ = 1.5406 Å) and Cu $K_{\alpha 2}$ (λ = 1.5444 Å), respectively; the (004) interplanar spacing d_{004} is estimated to be 1.3569 Å. On the other hand, the heat-treated sample [see

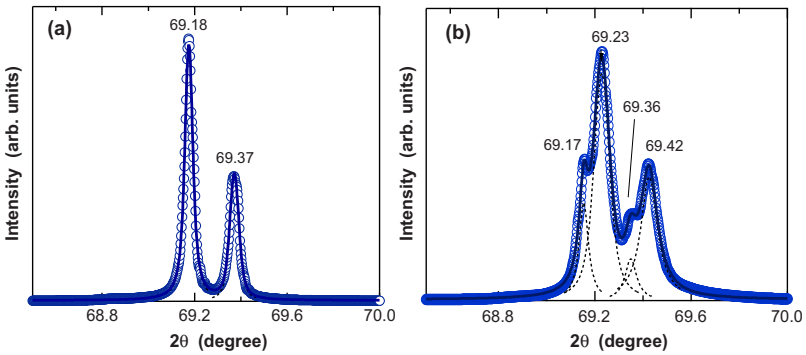

FIG. 2. (Color online) (a) Si(004)-Bragg reflection of the original (001) Si wafer. (b) Si(004)-Bragg reflection of the (001) Si wafer after heating at 1000 °C for 2 h under an Ar atmosphere in the presence of the MgO–MgB_2 composite. The open circles are the experimental data, the solid lines are the results of fitting using Voigt-type functions (dotted lines).

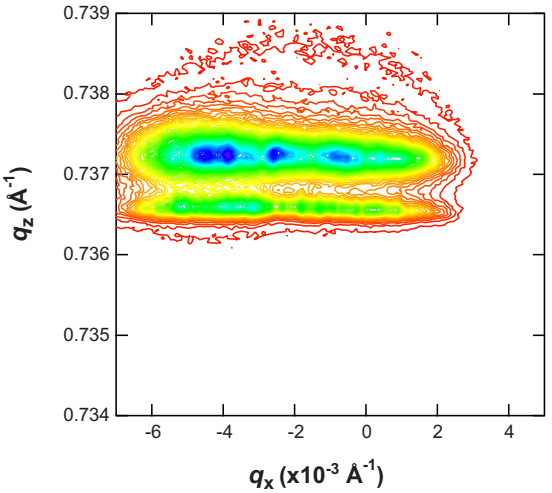

FIG. 3. (Color online) Reciprocal space map of the Mg-treated Si wafer. The data were obtained around the (004) Si lattice point and plotted in reciprocal coordinate q_x parallel to the [110] in-plane azimuth and q_z along the [001] direction.

Fig. 2(b)] exhibits four peaks at 2θ=69.16°, 69.23°, 69.36°, and 69.42°. The first (69.17°) and third (69.36°) peaks are comparable to the doublet of the Cu $K_{\alpha 1}$ and Cu $K_{\alpha 2}$ lines of the original Si wafer (d_{004}=1.3570 Å), whereas the second (69.23°) and the fourth (69.42°) peaks are attributed to another set of the Cu $K_{\alpha 1}$ and Cu $K_{\alpha 2}$ lines and are characterized by a slightly compacted d value (d_{004}=1.3561 Å).

To obtain further information on the lattice contraction, we next investigate the RSM of the Mg-treated Si sample. Figure 3 shows the RSM for the Mg-treated (001) Si wafer, with isointensity contour lines plotted in q_x along the [110] in-plane azimuth and q_z along the [001] direction. In the present (004) RSM, we see two peaks located at q_z=~0.7366 Å^{-1} (d_z=~1.357 Å) and ~0.7372 Å^{-1} (d_z=~1.356 Å), corresponding to the original Si lattice and the contracted one, respectively. Furthermore, both the peaks are highly scattered along the q_x direction, showing a typical mosaic-structured feature. This result demonstrates that the present Mg diffusion process induces not only lattice contraction but also variations in the orientation of the lattice planes parallel to the sample surface.

Figure 4 shows the cross sectional XRD pattern of the Mg-treated sample. A monochromatic x-ray beam of ~15 μm was irradiated on the surface cross-section of the sample; that is, a surface region of depth about ~15 μm can be exclusively investigated by this technique. We see from Fig. 4 that the XRD pattern consists of the diffraction peaks indexed to the cubic phase of Si (Joint Committee for Powder Diffraction Standard 27–1402) and that of MgO (Joint Committee for Powder Diffraction Standard 45–946). No diffraction peaks attributed to metallic Mg and any Mg- and B-related compounds, such as Mg_2Si and MgB_2, were found. Note also that all possible diffraction peaks of the cubic Si phase were observed, as in the case of powder diffraction patterns of polycrystalline Si. This indicates that as far as the [110] in-plane azimuth is concerned, the surface Si phase has no preferential orientation,[22] in harmony with the mosaic-structured Si lattice shown in Fig. 3. In the cross sectional

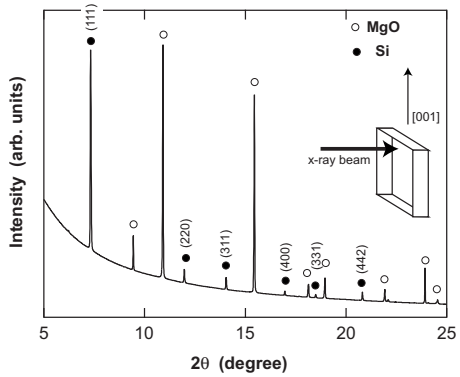

FIG. 4. A typical XRD pattern of a cross-sectional area of the Mg-treated Si wafer. Data were obtained with the microarea XRD system using a monochromatic x-ray beam (λ=0.400 085 Å) with a diameter of 15 μm. The x-ray beam was irradiated perpendicular to the cross section (slice plane) of the sample, namely, parallel to the [110] in-plane azimuth of the (001) Si wafer (see inset).

XRD pattern, respective Si-related diffraction peaks were composed of one component; the lattice parameter a estimated from the set of diffraction peaks (a=5.4278 Å) is slightly smaller than that of the normal cubic phase of Si (a=5.4309). The degree of contraction $\Delta a/a$ was −0.057%, which is almost comparable to that obtained from the two sets of Si(004) reflection ($\Delta d/d$=−0.066%) shown in Fig. 1. This indicates that only the contracted Si phase exists at the surface of the present Mg-treated Si sample.

B. EPMA analysis

The EPMA depth profile of the heat-treated sample is shown in Fig. 5. Both Mg and O were found in the region of ~6 μm thickness, whereas the B-concentration is virtually zero in the whole cross-sectional area investigated. The Mg-concentration tends to exceed the O-concentration with a decrease in depth from the top surface, indicating that a part of Mg is present in the form other than MgO in the near surface region. That is, Mg atoms are likely to diffuse into the Si lattice to form a Mg-doped Si layer with thickness of ~6 μm. Unfortunately, we cannot exactly estimate the concentration of Mg in Si because of a relatively large uncertainty (~40%) of the present EPMA depth profile analysis.

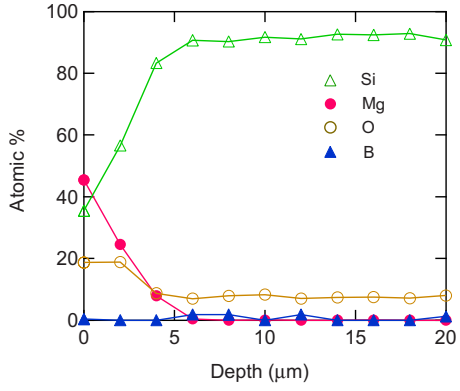

FIG. 5. (Color online) A typical EPMA depth profile obtained for a slice plane of the Mg-treated sample. Constant oxygen concentration (~10%) that is found in the depth region from ~6 to 20 nm results probably from a surface silica layer on the slice plane.

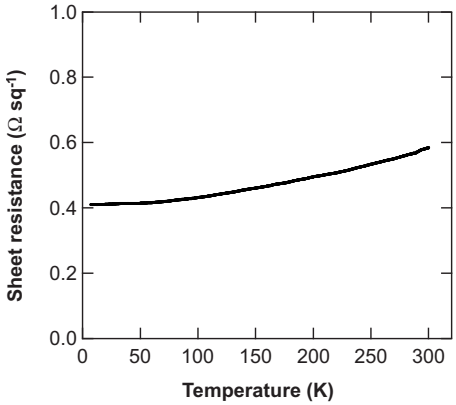

FIG. 6. Temperature dependence of the sheet resistance of the Mg-treated (001) Si wafer.

However, it can safely be said that the surface Si layer is heavily doped with Mg, containing at least a few atomic percent of Mg, that is, $\sim 1\times 10^{21}$ Mg cm^{-3}.

It is hence probable that the Mg-doped Si layer is responsible for the slight lattice contraction and mosaic grain region of silicon deduced from the XRD analysis mentioned in Sec. III A. Previously, local lattice relaxation of substitutional Mg in Si has been theoretically investigated.[23] According to the theoretical prediction,[23] the Mg–Si bond distance (2.352 Å) is very similar to the Si–Si bond distance (2.350 Å), implying that the Mg impurity in Si hardly affects the lattice constant. It appears that the prediction is inconsistent with the present observation. We should note, however, that the present Si lattice is only slightly modified ($\Delta d/d = \sim -0.06\%$) irrespective of the expected heavy doping. Furthermore, the Mg heavy doping may result in clustering of Mg atoms in the Si lattice, as in the case of the B atoms in heavily B-doped Si.[24] The effect of clustering of Mg atoms on the host lattice parameter is still unknown. As for the issues of the lattice parameter of the Mg-doped Si, further experimental and theoretical investigations will be required.

C. Electrical Properties

We next turn to electrical properties of the Mg-diffused sample. After the Mg-diffusion treatment, the original *p*-type and *n*-type Si wafers all exhibited *p*-type conduction characterized by low resistivity, illustrating that the diffused Mg atoms behave as substitutional acceptors. A typical example obtained for the Mg-diffused (originally *p*-type) Si wafers is as follows. At room temperature, the sheet resistance and the sheet carrier concentration were 5.8×10^{-1} Ω sq^{-1} and 4.5×10^{17} cm^{-2}, respectively, with a Hall mobility of 31.9 cm^2 V^{-1} s^{-1}. If we assume that the Mg ions are distributed uniformly in the Mg-diffused region with a thickness of ~ 6 μm, the resistivity and hole concentration are estimated to be $\sim 3\times 10^{-4}$ Ω cm and $\sim 7\times 10^{20}$ cm^{-3}. Furthermore, the sheet resistance shows a monotonic decrease with decreasing temperature down to 7 K (see Fig. 6), thus demonstrating a metal-like conducting behavior peculiar to a heavily doped degenerated semiconductor.

We should note that the above measurements were carried out without removing the surface insulating MgO layer. Thus, the observed values do not quantitatively represent the electrical properties of the conductive region of the sample. We, however, believe that the present measurements can capture the underlying electrical properties of the Mg-doped region of Si.

IV. DISCUSSION AND CONCLUSIONS

The present *p*-type conductivity is best interpreted if we assume that the doped-Mg atoms create substitutional acceptor levels in Si. As mentioned in the Introduction, however, Mg has been believed to occupy the tetrahedral interstitial site in silicon and form a deep-double-donor state.[5–11] These apparently contradicting observations presumably result from the fact that Mg can occupy interstitial or substitutional position depending on the sample preparation condition, as has been indeed suggested by several researchers.[12,13] Thus, the following question naturally arises: what is the main factor that governs the position and the concentration of Mg in silicon?

As pointed out in Sec. II, most of the previous studies employed the sandwich technique to diffuse Mg into Si.[5–7,11] This techniques inevitably accompanies the formation of Mg_2Si because of the thick magnesium film between two silicon substrates. We assert that once the stable Mg_2Si phase is formed at the Mg/Si interface, further thermal diffusion of magnesium into silicon will assist the crystal growth of Mg_2Si rather than promote an introduction of Mg into Si to create the Mg-related impurity sites. We hence suggest that the presence of the Mg_2Si phase will not raise but will lower the solubility of Mg in Si, forming only a small amount of interstitial donor levels.

If the above assumption is valid, solubility of Mg in Si can be increased when Mg diffusion is carried out in such a condition as to prevent the formation of Mg_2Si. As demonstrated above, the Mg vapor environment created by the thermal decomposition of MgB_2 indeed satisfies the above condition. The resulting Mg vapor pressure [$p_{Mg}\sim 10^{-3}$ bar at 1000 °C (Refs. 15 and 16)] is low enough to suppress the formation of the silicide phase but is high enough to induce Mg diffusion into Si. We should note, however, that metallic Mg cannot be used as an evaporation source for the present purpose because of its high vapor pressure ($p_{Mg}\sim 10$ bar at 1000 °C).[15,25] We indeed confirmed that Mg_2Si was formed at the surface of the Si substrate, as in the case of the sandwich diffusion technique, when we used metallic Mg and Si as an evaporation source and substrate, respectively (see Fig. 7). After removing the surface Mg_2Si layer, we found that the original *p*-type Si wafer changed to *n* type with high resistivity ($\sim 10^3$ Ω cm). These results further corroborate our assumption that the formation of Mg_2Si suppresses the solubility of Mg in Si, giving rise only to Mg interstitials.

Thus, we can conclude that as long as the Mg_2Si phase is not present, the thermal diffusion of Mg into Si results in substitutional Mg acceptors; the concentration of substitutional Mg can be raised up to $\sim 10^{20}$–$\sim 10^{21}$ cm^3, even yielding the degenerate *p*-type semiconductor. If the Mg_2Si

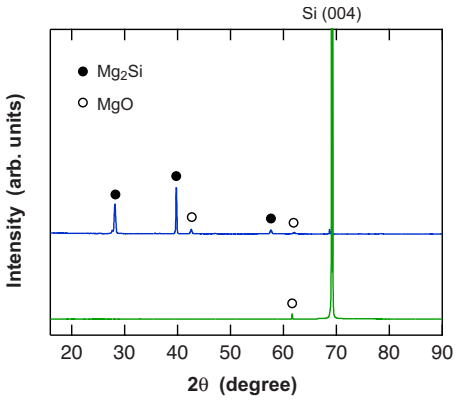

FIG. 7. (Color online) XRD patterns of the (001) Si wafer after heating at 1000 °C for 2 h under an Ar atmosphere in the presence of $MgO-MgB_2$ (lower) and metallic Mg (upper).

phase coexists, the solubility of Mg in Si becomes low ($\sim 10^{15}$ cm) only to form interstitial donor levels. That is, heavily magnesium doped "metallic" silicon is obtained by carefully controlling the vapor pressure of Mg. The present results will attract renewed interest in group-II impurities in Si in view not only of semiconductor-based technologies but also of a recently investigated metal-insulator transition of group-IV semiconductors.[26]

[1]R. K. Crouch, J. B. Robertson, and T. E. Gilmer, Jr., Phys. Rev. B **5**, 3111 (1972).
[2]J. B. Robertson and R. K. Franks, Solid State Commun. **6**, 825 (1968).
[3]J. M. Herman III and C. T. Sah, J. Appl. Phys. **44**, 1259 (1973).
[4]A. C. Wang, L. S. Lu, and C. T. Sah, Phys. Rev. B **30**, 5896 (1984).
[5]J. E. Baxter and G. Ascarelli, Phys. Rev. B **7**, 2630 (1973).
[6]A. L. Lin, J. Appl. Phys. **53**, 6989 (1982).
[7]R. K. Franks and J. B. Robertson, Solid State Commun. **5**, 479 (1967).
[8]L. T. Ho and A. K. Ramdas, Phys. Rev. B **5**, 462 (1972).
[9]E. Ohta and M. Sakata, Solid-State Electron. **22**, 677 (1979).
[10]M. Kleverman, K. Bergman, and H. G. Brimmeiss, Semicond. Sci. Technol. **1**, 49 (1986).
[11]A. L. Thilderkvist, M. Kleverman, and H. G. Grimmeiss, Phys. Rev. B **49**, 16338 (1994).
[12]N. Baber, L. Montelius, M. Kleverman, K. Bergman, and H. G. Grimmeiss, Phys. Rev. B **38**, 10483 (1988).
[13]S. Froyen and A. Zunger, Phys. Rev. B **34**, 7451 (1986).
[14]*Binary Alloy Phase Diagrams*, 2nd ed., edited by H. Okamoto, P. R. Subramanian, and L. Kacprzak (ASM International, Materials Park, OH, 1990), Vol. 1, pp. 498–500.
[15]S. Brutti, A. Ciccioli, G. Balducci, G. Gigli, P. Manfrinetti, and A. Palenzona, Appl. Phys. Lett. **80**, 2892 (2002).
[16]G. Balducci, S. Brutti, A. Ciccioli, G. Gigli, P. Manfrinetti, A. Palenzona, M. F. Butman, and L. Kudin, J. Phys. Chem. Solids **66**, 292 (2005).
[17]V. Sundaram, K. V. Logan, and R. F. Speyer, J. Mater. Res. **12**, 2657 (1997).
[18]Y. B. Zhang, M. Zeng, Z. S. Gao, J. Liu, H. M. Zhu, and S. P. Zhou, J. Supercond. Novel Magn. **22**, 729 (2009).
[19]We can also use pure MgB_2 to synthesize Mg-doped silicon. However, the MgB_2-MgO composite is more preferable than MgB_2 for practical purposes since the raw materials, Mg and B_2O_3, are easily commercially available.
[20]P. F. Fewster, Crit. Rev. Solid State Mater. Sci. **22**, 69 (1997).
[21]E. Koppensteiner, G. Bauer, H. Kibbel, and E. Kasper, J. Appl. Phys. **76**, 3489 (1994).
[22]However, the relative peak intensities of the Si-related peaks are not identical to those of the reported powder diffraction pattern of cubic silicon, implying that orientations of the mosaic-structured lattice are not completely random in the q_x direction.
[23]D. Sasireka, E. Palaniyandi, and K. Iyakutti, Int. J. Quantum Chem. **99**, 142 (2004).
[24]A. Vailionis, G. Glass, P. Desjardins, David G. Cahill, and J. E. Greene, Phys. Rev. Lett. **82**, 4464 (1999).
[25]*Selected Values of Thermodynamic Properties of the Elements*, in edited by R. Hultgren, P. J. Desai, D. T. Hawkins, M. Gleiser, K. K. Kelly, and D. Wagman (American Society of Metals International, Metals Park, OH, 1973).
[26]V. H. Crespi, Nature Mater. **2**, 650 (2003); X. Blase, E. Bustarret, C. Chapelier, T. Klein, and C. Marcenat, *ibid.* **8**, 375 (2009).